Study on the Hydrogeological Characteristics of the Roof Limestone Aquifer After Mining Damage in Karst Mining Areas

Xianzhi Shi , Guosheng Xu * , Ziwei Qian , Weiqiang Zhang

Posted Date: 6 June 2025

doi: 10.20944/preprints202506.0461.v1

Keywords: Karst mining area; Mining-induced damage; Specific yield; Simulation experiment; Research

 doi:10.20944/preprints202506.0461.v1

Article

Study on the Hydrogeological Characteristics of the Roof Limestone Aquifer After Mining Damage in Karst Mining Areas

Xianzhi Shi [1,2], Guosheng Xu [3], Ziwei Qian [1] and Weiqiang Zhang [1]

[1] School of Resources and Earth Science, China University of Mining and Technology, Xuzhou 221116, China
[2] Guizhou Yuxiang Mining Group Investment Co.. Ltd.，Bijie 551800, China
[3] College of Mining Engineering, Guizhou University of Engineering Science, Bijie 551700, China
* Correspondence: Guosheng Xu, Email: jzxgsheng@126.com

Abstract: In order to study the phenomenon of abnormal water burst in deep working faces during the production process of coal mines in karst landform mining regions in Guizhou Province, project researchers collected hydrogeological data from the exploration and production period of the Xinhua mining region in Jinsha County, Guizhou Province. Using ground and underground drilling, geophysical exploration techniques, empirical formulas, indoor material simulations methods, the hydrogeological evolution characteristics of the Changxing Formation limestone in the mining region after the mining damage of the coal bed 9 were studied. The research results indicate that the ratio of the height of the roof failure fracture zone measured by numerical simulation and ground borehole to the mining height is greater than 25.78 times, far greater than the empirical formula calculation value of 13.0-15.8. After the mining the underlying coal bed 9, abnormal water rich area developed in the Changxing Formation limestone, and the mining damage fractures connected the original dissolution fissures and karst caves within the limestone, resulting in the weak water rich (permeable) aquifer of the Changxing Formation limestone becoming a strong water rich (permeable) aquifer, which became the water source for mine water burst. Furthermore, Over time, the voids in the Changxing Formation limestone after mining damage are gradually filled with various substances, resulting in a decrease in water storage space and connectivity, the specific yield decreases with the increase of water burst time and the interval between the cessation of mining in the supply area, and the correlation coefficient R is 0.964, indicating a high degree of correlation between the two.

Keywords: karst mining area; mining damage; simulation experiment; specific yield

1. Introduction

Guizhou Province is the main area of coal mining in the karst region of southwestern China, and Jinsha County is one of the important coal mining areas in the province. In the early stages of mining in karst mining areas in Guizhou Province, atmospheric precipitation serves as the primary recharge source during mine operation [1–7]. In the Xinhua mining region the Changxing Formation limestone outcrops extensively on the surface, and the limestone can directly receive atmospheric precipitation and indirectly fill the stope with water. A clear correlation exists between mine water inflow and atmospheric precipitation [5,8]. The Changxing Formation limestone in the mining area is a weakly water-rich (permeable) aquifer, with good water rich properties in local structures, dissolution fissures, and karst caves. The formation can serve as a channel for rainfall to supply deep mining stope. Although there is a significant difference in the inflow of underground water between rainy and dry seasons in mines located near coal bed outcrops within the mining area, there have been no occurrences of water burst in the early stages of mining [2,4]. Because of the expansion of goaf areas and the increasing mining intensity of multiple coal mines within the mining region, frequent roof

 doi:10.20944/preprints202506.0461.v1

water burst has begun to occur in mines in which deep coal beds are mined, causing the working face to be flooded at one point and resulting in accidents causing casualties due to water burst [9–11].

For studying the mechanism of water burst, various scholars at research institutions, colleges and universities have focused mainly on the Permian and Jurassic sandstone aquifers in the northern part of the region; they have studied the mechanism of roof water burst [12–15] and have conducted to study the mechanism or treatment of water burst in the bottom limestone aquifer [16–18]; however, no researchers have investigated the mechanism of roof water burst in limestone. The water storage characteristics of limestone aquifer mainly consist of dissolution fissures and karst caves, which are significantly different from those of sandstone aquifer mainly consisting of fractures. Therefore, the above research results cannot clarify the failure characteristics and water burst mechanism of Changxing Formation limestone. Some scholars or engineering technicians have used drilling [19] methods to study the characteristics of the recharge of the water source and aquifer in the top plate of the stope, and they have identified the characteristics of the water source of water burst and aquifer of the top plate, thereby providing a foundation for taking water hazard prevention and control measures in mines. However, since these studies were conducted under the condition that the top plate was not affected by mining, they cannot explain the water-filling characteristics of the aquifer after damage during mining. Many studies have been conducted on the hydrogeological conditions of the aquifer in the known coal bed roof during mining [1,4,9,10]. However, few scholars and engineering technicians have investigated the phenomenon of water burst in the working face of the Changxing Formation limestone-roof in the Xinhua mining region in northern Guizhou, where the water richness is low and no water burst occurred during the early stage of mining. Many scholars, such as Shuyuan Xu, are conducting research on fracture zones that conduct roof water, such as Jinjun Li et al. [20], Jiabo Xu et al. [21]. Due to the fact that the simulated coal bed roof is predominantly consists of sandstone, sandy mudstone and other rock types, with no developed limestone strata and few coal beds, it cannot be used to accurately predict the height of water-conducting fracture zones in the coal bed roof and coal bed in the Xinhua region. However, in previous research on water hazards in the limestone of the Changxing Formation on the roof, the main focus has been on water during bed separation [1,3,22,23]. Research on the changes in the hydrogeological conditions of Changxing Formation limestone after coal mining and damage is lacking, and research on water channels is sparse; thus, this previous research cannot reasonably clarify the mechanism of water burst in Changxing Formation.

The paper collected and analyzed a large amount of geological and hydrogeological data from the Xinhua mining region. Using empirical formulas, material simulations, and ground borehole detection, it investigated the damage mechanism and height of roof after coal bed mining beneath the Changxing Formation in the Xinhua karst mining region; Additionally, the study examinged the changes in hydrogeological conditions of Changxing Formation limestone before and after mining-induced damage, and calculated the specific yield of Changxing Formation limestone after mining damage using on-site measured data. The research results provide a theoretical basis and practical reference for the treatment of roof limestone water inrush hazards in mines with similar hydrogeological conditions.

2. Materials and Methods

2.1. Overview of the Research Region

2.1.1. General Overview of the Mining Region

The Xinhua mining region (referred to as the mining region in this study) is situated within the territory of Jinsha County, Bijie City in Guizhou Province (Figure 1), and southwest of Jinsha County, on the northwest wing of the Jinsha Qianxi syncline, with a mining area of approximately 220 km^2. There are currently 22 pairs of producing and developing coal mines in the mining region, with single-well design production capacities between 300000 and 1.5 million tons per year and single-well field areas between 1.81 and 90.02 km^2.

 doi:10.20944/preprints202506.0461.v1

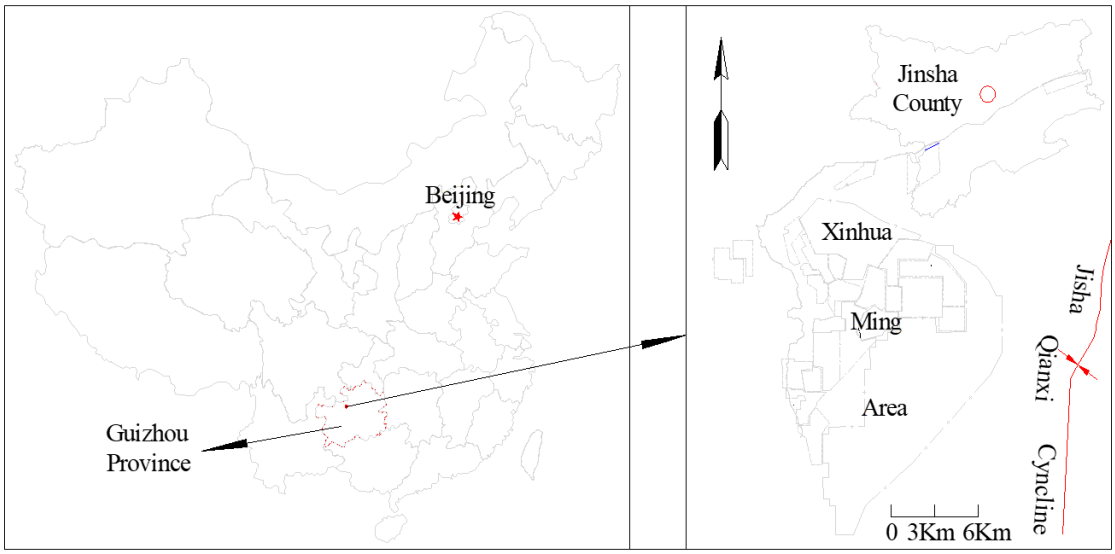

Figure 1. Location of the Xinhua mining region.

2.1.2. Geology of the Mining Region

The main strata that impact the mining of coal-bearing stratum within the mining region, from oldest to youngest, include the middle Permian Maokou Formation (P_2m), upper Permian Longtan Formation (P_3l) , Changxing Formation (P_3c), Lower Triassic Yelang Formation (T_1y) and Maocaopu Formation (T_1m); and Quaternary strata (Q). Among these strata, the coal-bearing stratum is exclusively hosted in the Permian Longtan Formation (P_3l).

The overall strata of the mining area have a monocline structure, with local undulations forming secondary fold structures. The inclinations of the formation in the mining area are 65°–155°, with dip angles of 0°–27°, primarily 5°–10°. The coal mines within the mining region have exposed small faults with varying decreases in the production and construction areas, and some mines have revealed collapsed columnar structures.

The Longtan Formation (P_3l) within the mining region severs as a coal-bearing formation that is composed of mainly gray to grayish-black thin-to-medium-bedded siltstone, sandy mudstone, and argillaceous sandstone interbedded with fine sandstone, calcareous mudstone, and 4–7 layers of limestone and argillaceous limestone. It hosts 12–15 coal beds, including 2–6 mineable coal beds, among which the $4^{\#}$, $9^{\#}$, and $15^{\#}$ coal beds are the principal mining coal beds in most mines. The coal bed 9 exhibits a thickness varying between 0.59–9.95 m (average 2.77 m), and is the main mined coal bed in most mines in the mining area.

2.1.3. Hydrogeological Conditions of Mining Region

The principal aquifers in the mining region consist of the Yulongshan Member (T_1y^2) limestone of the Triassic Yelang Formation, the Permian Changxing Formation (P_3c) limestone, and the Permian Maokou Formation (P_2m) limestone (Figure 2). The Yulongshan member (T_1y^2) limestone of the Triassic Yelang Formation is the primary aquifer in this mining region, with a thickness varying between 176.62–248.3 m (average 211.92 m). The karst development of this aquifer varies greatly, and is classified as weakly to strongly water-bearing aquifers. The Yulongshan member limestone is separated from the underlying coal-bearing strata by the Shapuwan member (T_1y^1) aquitard, with a thickness varying between 7.45–21.11 m (average 14.91 m). The aquifers that can directly recharge water to the Longtan Formation coal-bearing strata are limestone of the overlying Changxing Formation and the underlying Maokou Formation. The Changxing Formation (P_3c) limestone is in integrated contact with the Longtan Formation, with a thickness varying between 17.85–61.72 m (average 39.00 m) (Figure 3). 13 sets of pumping test data indicate that the aquifer is a weak water rich aquifer. The Maokou Limestone in the mining area has a thickness exceeding 200m, with a specific capacity ranging from 0.000915 to 0.148144 L/s·m. It is a weak to moderate water rich aquifer.

 doi:10.20944/preprints202506.0461.v1

The coal-bearing strata of the Longtan Formation (P_3l) have somewhat numerous water layers and aquicludes, and the various lithologies within the strata are prone to mudification when exposed to water, which can block water-conducting channels.

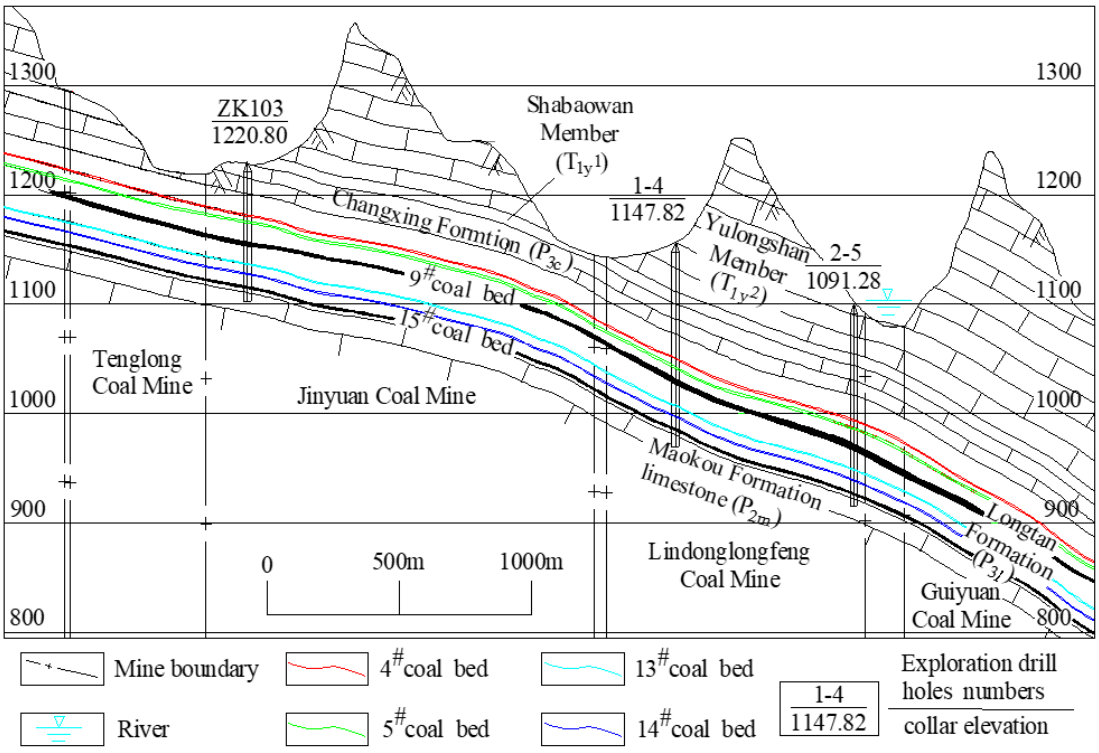

Figure 2. Geological section of the mining region.

The main sources of groundwater supply in the mining area are surface rivers and atmospheric precipitation, which infiltrate into the deep through surface outcrops for replenishment. The roof of the coal bearing strata is mainly supplied by the limestone water of the Changxing Formation, and can indirectly receive the limestone water supply of the Yulongshan Formation in structural development area. The floor is mainly supplied by the limestone water of the Maokou Formation.

 doi:10.20944/preprints202506.0461.v1

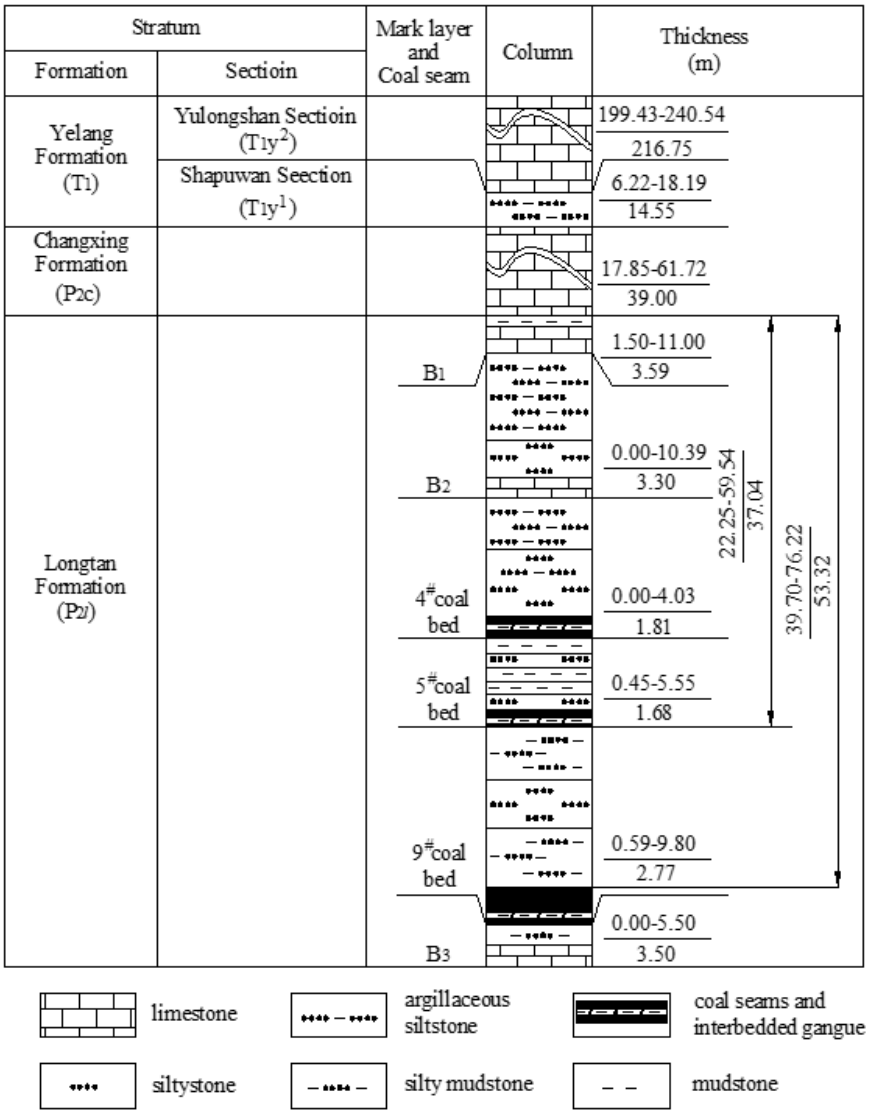

Figure 3. Composite stratigraphic column of the coal measures in mining region.

According to the exploration data from each mine field in the mining region and the hydrogeological data revealed during the period of production of the coal mines, the hydrogeological conditions of all coal mines in the mining region are similar. On the basis of the comprehensive analysis of exploration data from each coal mine in the mining region, the coal deposit exploration type in the mining region is the first type in the third category, which is the type referring to deposits with water-filled karst and simple hydrogeological conditions.

Since June 2016, when the 10903 working face of the coal bed 9 in the Guiyuan Coal Mine began to experience water burst, mines such as the Linhua Coal Mine, Jinji Coal Mine, Tenglong Coal Mine, Lindonglongfeng Coal Mine, and Anshenglongfeng Coal Mine in the mining region have experienced water burst from the roof of the coal bed 9 working face [5,8–10], seriously affecting mine safety production. According to the mining data of the coal bed 9 working face within these mines, the seam-mining heights of the coal bed 9 are between 1.5 and 3.4 meters. During nomal production, the normal water inflow of the working face is between 20 and 220 m^3/h, and the sudden water inflow values are generally between 80 and 800 m^3/h.

2.2. Geological Data Collection and Research

Before and during the development of the mining region, researchers in the country carried out large-scale geological surveys and constructed many survey boreholes. After the division of each mining field, workers in each coal mine carried out exploration work in the mine and constructed

 doi:10.20944/preprints202506.0461.v1

refined exploration drill holes; the exploration level was reached in each mining field, and reliable geological, hydrogeological and other geological technical data were provided for mine construction and production. Researchers collected geological data from 22 pairs of producing and developing coal mines at different stages of production within the mining area and analyzed the data. They studied the characteristics of geological and structural development and hydrogeological conditions via 348 boreholes already constructed in the mining area. Researchers recorded 10 cases of water burst from the Changxing Formation limestone caused by faults and 12 cases of water burst from normal geological blocks (see Table 1) and collected relevant data, such as the water burst location, mining height, structure of the water burst point, date of water burst, burial depth and elevation at the water burst location, and maximum water burst volume for all working faces of the all coal mines. The transient electromagnetic method was conducted to detect abnormal water-rich changes in the top plate of Changxing Formation limestone affected by mining (shallow, deep, and near-cut faces have all been mined) and unaffected by mining. The specific yield of the Changxing Formation limestone after mining-induced damage was investigated using static water-burst recharge water data.

Table 1. Statistics of water burst points in mines in the mining region.

Serial number	Mine	No. of water burst working face	Location of water burst	Mining height (m)	Structure of the water burst point and working face conditions	Water burst time (year, month, day)	Elevation (burial depth)of water burst point (m)	Maximum water burst influx (m^3/h)	notes
1	Linhua Coal Mine	2093	Stop mining line location	3.3	Fault	2012.3.17	1041.3 (338.7)	200	
2		20910	673 m away from the open-off cut	3.4	Normal stratigraphic block	2017.10.10	916 (374.8)	96	
3		20912	523 m away from the open-off cut	3.4	Normal stratigraphic block	2016.1.10	866 (379.1)	210	
4		20917	232 m away from the open-off cut	3.3	Normal stratigraphic block	2019.1.10	833.6 (491.6)	86	
5		10901	89 m away from the open-off cut	3.3	Normal stratigraphic block	2019.11.17	829.5 (447.5)	310	
6	Guiyuan Coal Mine	10903	276 m away from the open-off cut	3.0	Near the fault	2016.6.16	783 (367)	280	T-1
7		10901-1	80 m away from the open-off cut	2.5	Between two faults	2019.2.25	833 (415)	160	T-2
8			74 m away from the open-off cut	3.0	Near the fault	2020.3.30	747 (421)	229	T-3
9		10905	143 m away from the open-off cut	3.0	Near the fault	2020.5.12	751 (436)	150	T-4
10			425 m away from the open-off cut	3.0	Near the fault	2020.11.8	776 (433)	290	T-5

 doi:10.20944/preprints202506.0461.v1

11	Jinji Coal Mine	10908	247 m away from the open-off cut	3.0	Normal stratigraphic block	2021.10.13	808 (394)	210
12			341 m away from the open-off cut	3.0	Normal stratigraphic block	2022.2.14	807 (439)	80
13		2093	161 m away from the open-off cut	2.5	Near the fault	2019.7.15	728.5 (431.5)	150
14			237 m away from the open-off cut	2.5	Near the fault	2019.11.23	729.8 (432.6)	470
15			270 m away from the open-off cut	2.5	Near the fault	2019.12.10	730.9 (439.4)	350
16		1905	41 m away from the open-off cut	2.8	Normal stratigraphic block	2018.12.20	877.5 (366.1)	200
17	Lindongl ongfeng Coal Mine	5914	202 m away from the open-off cut	2.4	Expose faults	2019.7.22	979.3 (146.2)	160
18			365 m away from the open-off cut,	2.4	Normal stratigraphic block	2020.3.24	977.8 (127.4)	210
19	Tenglong Coal Mine	10901	163 m away from the open-off cut,	2.3	40 m away from the nearby working face	2020.4.19	1047.3 (342.7)	80
20			536 m away from the open-off cut	2.3	27 m away from the nearby working face	2020.11.11	1047.4 (350.1)	800
21	Anshengl ongfeng Coal Mine	10903	465 m away from the open-off cut	2.5	Normal stratigraphic block	2022.6.19	993.4 (274.1)	Collapse of water and yellow mud
22		10905	27.8 m away from the open-off cut	2.8	Normal stratigraphic block	2023.4.12	774 (335.5)	578

2.3. Research Methods for Roof Damage Height

2.3.1. Calculation of the Empirical Formula

Theoretical calculations of the height of development of water-conducting fracture zones have revealed a large number of statistical data around China. Researchers have used statistical methods to study and measure the height of development of water-conducting fracture zones under various rock settings. On the basis of the presence of coal beds and their roofs within the research region, an empirical formula to determine the height of development of water-conducting fracture zones has been derived. The formula to calculate the height of the water-conducting fracture zone as specified in the "Code for Retaining Coal Pillars and Coal Mining in Buildings, Water Bodies, Railways, and Main Mines" [24] was used to calculate the height of the water-conducting fracture zone. The rocks between the coal bed 9 and the Changxing Formation limestone within the mining region are

 doi:10.20944/preprints202506.0461.v1

composed of mainly argillaceous siltstone, silty mudstone, siltstone, etc. (Figure 3), with average compressive strengths of 35.74 MPa, 30.75 MPa, 43.90 MPa, 46.73 MPa, and 53.72 MPa, respectively. The strata between the coal bed 9 and the Changxing Formation limestone are primarily medium-hard rocks (the uniaxial compressive strength of the rock is 20-40 MPa, and the rock types are sandstone, argillaceous limestone, sandy mudstone, and mudstone). Therefore, the empirical formula to calculate the height of the water-conducting fracture zone used in this study is as follows:

$$H_{li} = \frac{100\sum M}{1.6\sum M + 3.6} + 5.6 \quad (1)$$

Where H_{li} is the height of development of the water-conducting fracture zone (m), and M is the cumulative thickness of the coal bed (m).

2.3.2. Simulation of the Water-Conducting Fracture Zone Height

The simulation experiment of similar materials is an important scientific research method for solving geological engineering problems in coal mines. It is to create a model in the laboratory that is similar to the geological strata in the research area using similar materials. With the help of the model, the changes in the simulated strata during coal bed mining can be observed, and the height of roof rock collapse and fracture development can be inferred after coal bed mining, thereby obtaining the mining failure height, strata movement law, and stress distribution state in mine production. This research method has the advantages of intuitiveness, simplicity, economy, speed, and short experimental period. Therefore, on the basis of the characteristics of the distribution of water burst mines in the mining region, a similar material-simulating experiment was conducted on the 10901-1 water burst working face of the Guiyuan Coal Mine. The 10901-1 working face is located in the first mining district of the Guiyuan Coal Mine. The north side border of the working face is the deep 10903 goaf, the south and east sides are the mine boundaries, and the west side is the 10901 goaf. The corresponding surface for this working face is composed of barren mountains without rivers or lakes, or other water bodies. The 10901-1 working face is an irregular polygon (see Figure 4) with an average strike length of 630 m and a dip length of 110 m. The average dip angle of the coal bed is 7°, and the mining thickness of the working face is 3.00 m. The average burial depth of the 9 coal bed 9 within this working face is 389 m, the thickness of the Changxing Formation limestone aquifer on its roof is 39.48 m, and the average distance between the floor of the Changxing Formation and the coal bed 9 is 42.81 m.

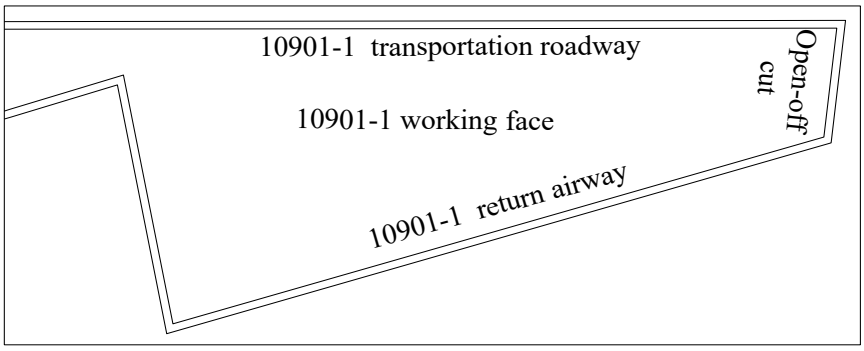

Figure 4. Layout of the 10901-1 working face in the Guiyuan Coal Mine.

Based on the mining conditions of the coal bed in the working face, a similar model of 250 cm (length) × 20 cm (width) × 140 cm (height) for the simulation was established at a ratio of 1:150. On the basis of the empirical values of the height of the water-conducting fracture zone mentioned above, the rock layer of interest in the model is determined to be the rock layer below the limestone in the Yulongshan member. Owing to the limited height of the experimental equipment, the strata from the top rock layer to the surface is implemented as a load. The model is illustrated in Figure 5.

 doi:10.20944/preprints202506.0461.v1

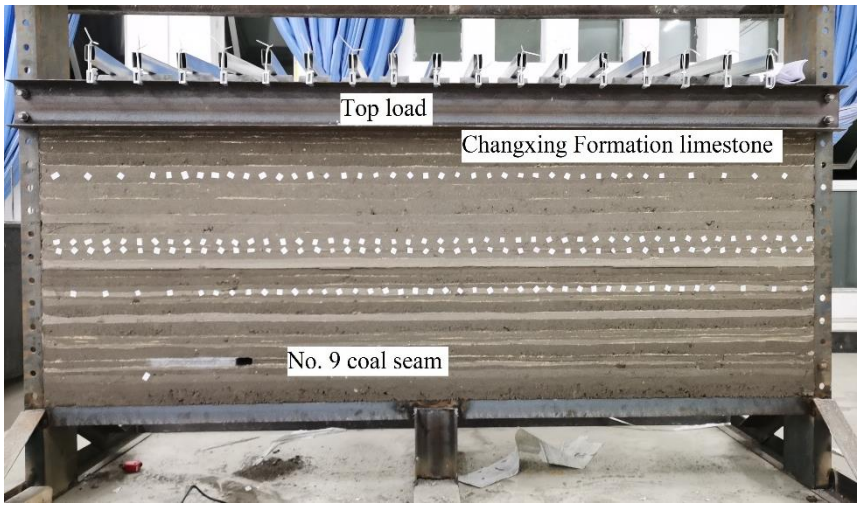

Figure 5. Water-conducting fracture zone simulation model.

The materials selected for the test model are fine sand, which are used as aggregates; calcium carbonate and gypsum, which are used as bonding materials; and mica powder, which is used as an interlayer weak surface material. The fine sand contents in various rock types are between 30% and 70%, the calcium carbonate contents are between 12% and 49%, and the gypsum contents are between 9% and 30%. The mechanical parameters of coal beds and various types of rock strata, as well as the corresponding proportions of similar materials, are presented in Table 2.

Table 2. Proportions of similar simulated materials.

Lithology	Compressive strength of the model (KPa)	Ratio of materials	Proportion of material used (%)		
			Fine sand	Calcium carbonate	Gypsum
Siltstone	136	737	70	9	21
Limestone	154	455	40	30	30
Silty mudstone	100	755	70	15	15
Mudstone	91	473	40	42	18
Fine sandstone	113	373	30	49	21
Coal	45	773	70	21	9
Argillaceous siltstone	104	746	70	12	18

2.3.3. Ground Exploration via Drilling

After coal bed mining, the surrounding roof of the working face is damaged to form a circular crack circle. By using ground drilling, it is possible to investigate the water leakage situation and rock fragmentation of the fracture zone, thereby obtaining the development height of the water conducting fracture zone after coal bed mining [25]. To study the development height of water conducting fractures, during the later supplementary exploration process of the mine, two exploration boreholes, 601 and 602, were designed and constructed above the 2900 working face and 2905 goaf in the Guiyuan coal mine in the mining region. The hole positions were 17.1m and 8.5m away from the edge of the goaf, respectively, to explore the height of the water conducting fracture zone formed after the mining of the coal bed 9 (Figure 6).

 doi:10.20944/preprints202506.0461.v1

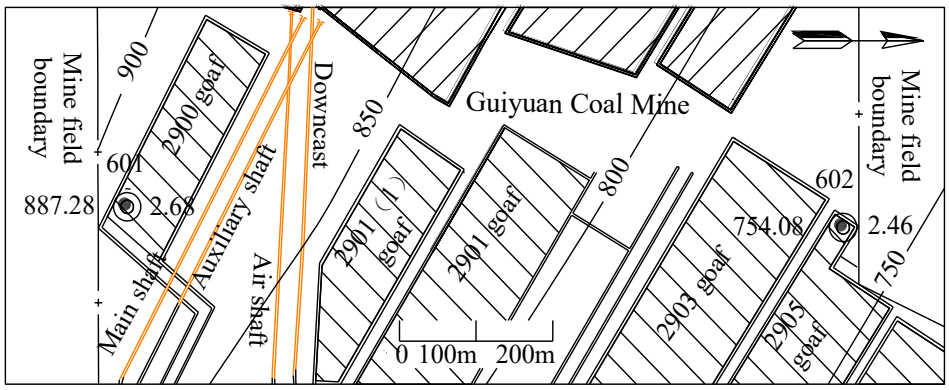

Figure 6. Layout of boreholes for surface exploration of the water conducting fracture zone height.

The 2900 and 2905 working faces are located in the second mining district of the Guiyuan Coal Mine, with inclined lengths of 108 m and 136 m, respectively. Fully mechanized mining technology is adopted for the working face, with full-height mining used once and with full-collapse method for roof management. The coal bed 9 was mined in the two working faces, with mining heights of 2.68 m and 2.46 m. The roof rock of the two working face is composed of mainly siltstone, silty mudstone, and argillaceous sandstone.

3. Study on the Damage Characteristics of Changxing Formation Limestone After Coal Bed Mining

3.1. Research on Mining-Induced Fracture Zone Height

3.1.1. Calculation of the Empirical Formula

The distances between the coal bed 9 in the mining region and the Changxing Formation limestone are 39.70 to 76.22 m (average 53.32 m). In wate-burst coal bed, The mining height of coal bed 9 varies between 2.3 and 3.4 m. According to Formula (1) calculation, the heights of the water-conducting fracture zones in the mining region are between 37.2 and 42.8 m. According to the results calculated by formula 1, combined with the distance between coal bed 9 and Changxing Formation and the data analysis in Table 3, the water conducting fracture zones in the most mines cannot develop into Changxing Formation limestone after the mining of coal bed 9 , and mining is unlikely to cause damage to Changxing Formation limestone. Therefore, further research on the development characteristics of the water conducting fracture zone in the coal bed 9 of the mining region is necessary to explain the mechanism of water burst from the Changxing Formation limestone after mining damage.

Table 3. Statistical table of height calculation of water-conducting fracture zones in some water burst working face.

Coal mine	Linhua Coal Mine	Guiyuan Coal Mine	Jinji Coal Mine	Lindong longfeng Coal Mine	Tenglong Coal Mine	Ansheng longfeng Coal Mine
No. of water burst working face	10901	10908	1905	2914	10903	1905
Mining height (m)	3.3	3.0	2.8	2.4	2.5	2.8
Height of water conducting fracture zone（m）	42.8	41.3	40.3	37.9	38.5	40.3
Fracture Zone Height to Mining Height Ratio	13.8	13.0	14.4	15.8	15.4	14.4

 doi:10.20944/preprints202506.0461.v1

Distance between 9# coal bed and Changxing Formation limestone（m）	54.84	50.68	49.81	55.59	49.09	41.78

3.1.2. Results of the Simulation of Similar Materials

The coal bed was mined according to the experimental design, and the experiment showed the process and mechanism of roof failure after mining of coal bed 9. After mining from the open-off cut of the working face, the overlying roof rock layer loses the support of the underlying rock layer and undergoes bending deformation under self-weight stress. When the tensile strength of the rock layer reaches its limit, it breaks and forms a goaf caving zone. At this time, the roof mining fractures are mainly concentrated on both sides of the goaf boundary (see Figure 7 (a)). As the area of the goaf increases, the deformation caused by mining movement is transmitted from bottom to top, and mining fractures develop upwards. When the working face advanced to 89m, transverse fissures began to form at the bottom of the hard limestone layer in the Changxing Formation. The vertical fissures were controlled by the main roof and developed at a height that lagged behind the height of the transverse fratures. At this time, the height of the water conducting fracture zone was 19.8m (see Figure 7 (b)). When the working face advanced to a length of 106 meters, the fine sandstone main roof in the upper part of the goaf was broken, and the weak rock layer (forming a composite beam structure) in the upper part of the main roof experienced synchronous settlement. Afterwards, the transverse fissures at the bottom of the Changxing Formation limestone layer expanded, and the height of the vertical fissures gradually increased. The height of the water conducting fracture zone reached 33.2 meters, as shown in Figure 7 (c).

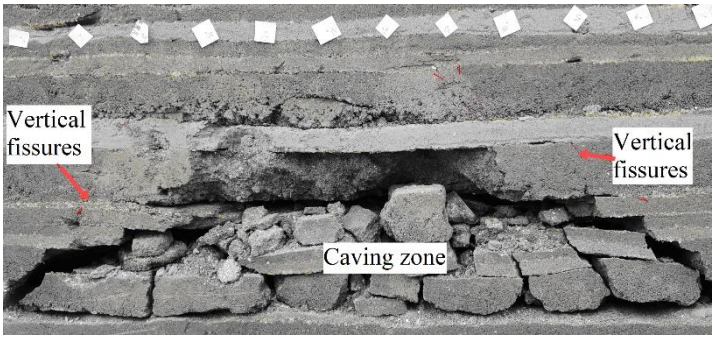

(**a**)

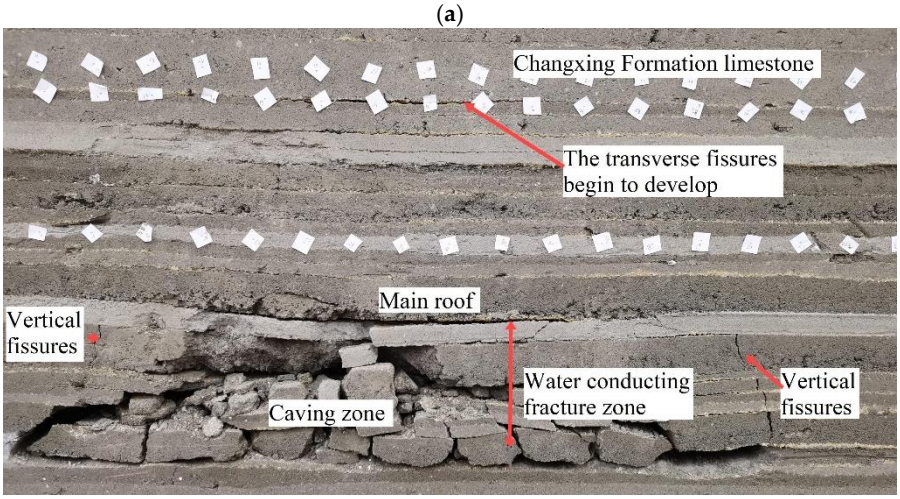

(**b**)

 doi:10.20944/preprints202506.0461.v1

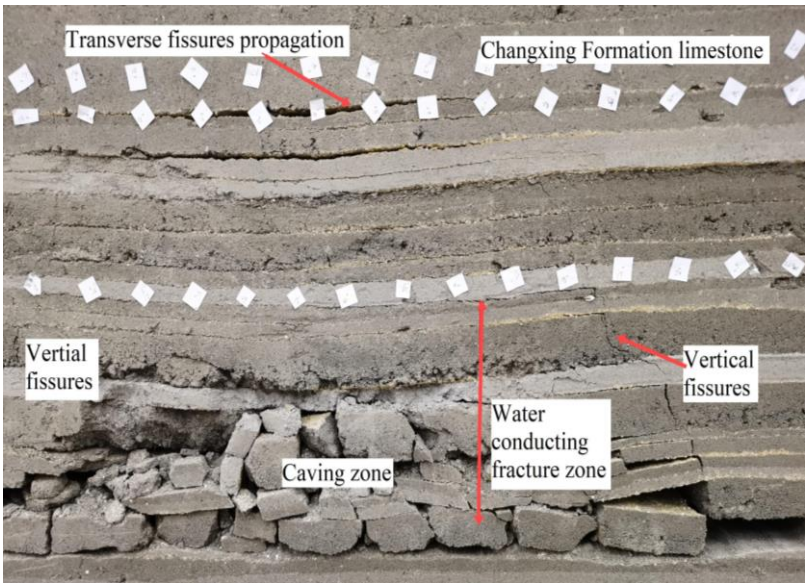

(c)

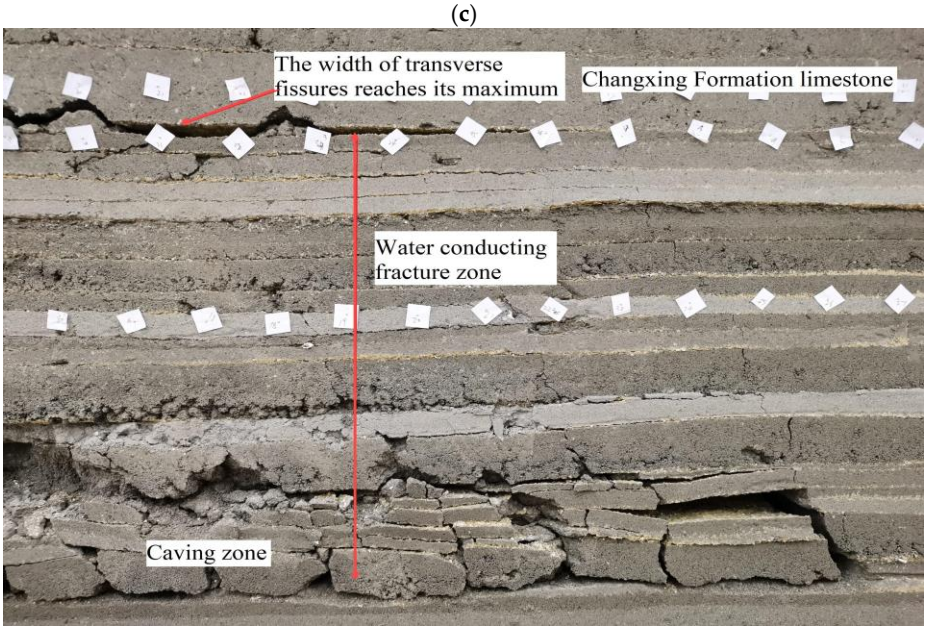

(d)

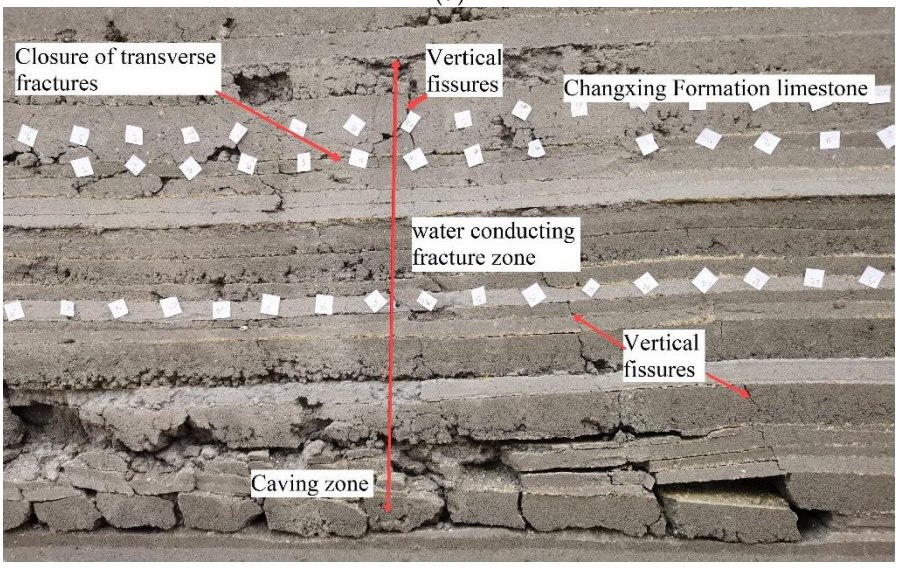

(e)

Figure 7. The damage mechanism diagram of the Changxing Formation limestone (Scale: 1:150) **(a).** Caving of the immediate roof in the goaf (working face advance distance 59m). **(b).** Formation of transverse fissures

 doi:10.20944/preprints202506.0461.v1

(working face advance distance 89m). **(c).** Elevation of mining-induced fractures and expansion of transverse fissures (working face advancement distance 106m). **(d).** The transverse fissures developed to their maximum width (working face advancement distance 150m). **(e).** The transverse fissures closure while the vertical fissures leap (working face advance distance 179m).

As the working face continues to advance to 150m, the width of the transverse fissures reaches its maximum width of 1.7m; Vertical fissures have also developed to the floor of Changxing Formation limestone floor, with a water conducting fracture zone height of 42.81m (see Figure 7(d)). Afterwards, the width of the transverse fissures gradually decreased. When the working face advanced to 179m, the length of the goaf reached the limit breaking distance of the limestone, and the Changxing Formation limestone fractured. The transverse fissures closed, causing the height of the water conducting fracture zone to jump into the Changxing Formation limestone body, as shown in Figure 7 (e). At this point, the vertical fissures far from the edge of the goaf have mostly closed, while those near the edge of the goaf remain open and developed into the middle-upper section of the Changxing Formation limestone. The height of the water conducting fracture zone was finally measured to be 77.33 m, with a ratio of 25.78 to the mining height. The water conducting fracture zone extended into the limestone of the Changxing Formation, resulting to its failure.

3.1.3. Ground Drilling Actual Measurement of Water Conducting Fracture Zone Height

During the supplementary exploration process during the normal production period of the mine, the 601 and 602 boreholes constructed at Guiyuan Coal Mine both exposed the Yelang Formation (T_1y), Changxing Formation (P_3c), and Longtan Formation (P_3l) strata, and terminated at the Maokou Formation (P_2m) limestone and the floor of the coal bed 9, respectively; the drilling depths are 345.11 m and 414.50 m, respectively. Two boreholes revealed the goaf of coal bed 9, and working face mining heights were 2.68 m and 2.46 m respectively. The distances between coal bed 9 and the Changxing Formation limestone are 41.2 m and 43.3 m, respectively. The exploration boreholes of the 601 and 602 water-conducting fracture zones revealed water leakage throughout the entire layer of the Shabaowan member of Yelang Formation (T_1y^1) and the limestone of Changxing Formation strata. The exploration results of these two boreholes indicate that at the edge of the goaf, the mining-damaged height has significantly increased, with the maximum height of the water-conducting fracture zone reaching exceeding 43.3 m, and the mining damage has affected the entire Changxing Formation limestone. The working faces of the Linhua Coal Mine, Tenglong Coal Mine, Guiyuan Coal Mine, Anshenglongfeng Coal Mine and other coal mines in the mining region have experienced water burst from the limestone roof the near the open-off cut, long-term stopping position, stress concentration area, etc., which verifies the accuracy of the borehole exploration results and related research results in this mining region [3,26].

3.2. Fault Re-Rupture

Faults can serve as both sources of water storage and channels for conducting water burst. Water burst in fault zones are one of the major hazards that threatens coal mine safety production [4,27,28]. When water burst occurs at the working face, the activation of faults can lead to the formation of unobstructed water channels, which is often an important factor leading to water burst. This is also an important reason why the working face does not experience water burst during roadway construction but rather during mining [29,30]. During the process of advancing the working face, the mining movement stress causes the rock mass stress within a certain range of the advancing direction of the working face to redistribute, forming a stress concentration zone. Owing to the disruption of the integrity of the rock layer caused by fault cutting, abnormal stress occurred in the fault zone during mining activities, resulting in sliding between the hanging wall and footwall of the fault, increased fractures between fault zones, and other phenomena, making the fault zone and fractures near the fault become water channels [31–37]. In such situation, the fault zone of the coal bed roof,

 doi:10.20944/preprints202506.0461.v1

fault-associated fracture zone, and water-conducting fracture zone of the roof are interconnected with the water-filled aquifer. This caused water inflow from the aquifer into the stope.

Near fault, owing to the damage caused by the fault, the fissures in the Changxing Formation limestone are more developed than those in normal geological blocks, and the water-rich properties of the limestone of Changxing Formation are relatively good. The combination of mining-induced fractures and zones of fault increases the connectivity among primary fractures, dissolution fissures, and karst caves in the Changxing Formation limestone. The superposition of their effects not only increases the water storage capacity of the Changxing Formation limestone in the goaf roof but also causes rapid and large water bursts in the working face. As the number of exposed faults in the working face increases, the frequency of water burst also increases, as shown in Table 1, water burst events caused by faults in the panel 10905 and 2093 in Guiyuan Coal Mine occurred three times respectively, which is far greater than the number of water burst in working faces of nomal geological blocks.

There are 22 water burst events in the mining region so far (Table 1), among which 10 are located near faults, accounting for 45.45% of total. The water burst fault exposed in the mining region has a drop of 0.6-2.5m, and the distance between the water burst point and the fault ranges from 7.0-60.0m (see Table 4). The water burst volume is significantly correlated with the distance between the water burst point and the fault (see Figure 8 and Formula 2), with a correlation coefficient R of 0.61. Before water burst at working face, there were dripping and water seepage phenomena on the roof, accompanied by a significant increase in roof pressure and pressure from the old roof. There have been 10 water burst events in the Guiyuan Coal Mine within the mining region, among which 8 water burst points located near the working face fault. The distances between the water burst points and the fault vary from 16.6 to 60.0 m (Figure 9), and the water burst volumes range from 150 to 470 m^3/h.

Table 4. Statistical data on water burst volume and distance from water burst points to faults.

Serial number	1	6	7	8	9	10	13	14	15	17
Mine	Linhua Coal Mine				Guiyuan Coal Mine					Lindonglongfeng Coal Mine
No. of water burst working face	2093	10903	10901-1		10905			2093		5914
Distance from water burst points to faults (m)	7.0	51.0	41.4	17.2	29.0	18.3	16.6	60.0	36.9	24.9
Maximum water burst influx (m^3/h)	200	280	160	229	150	290	150	470	350	160

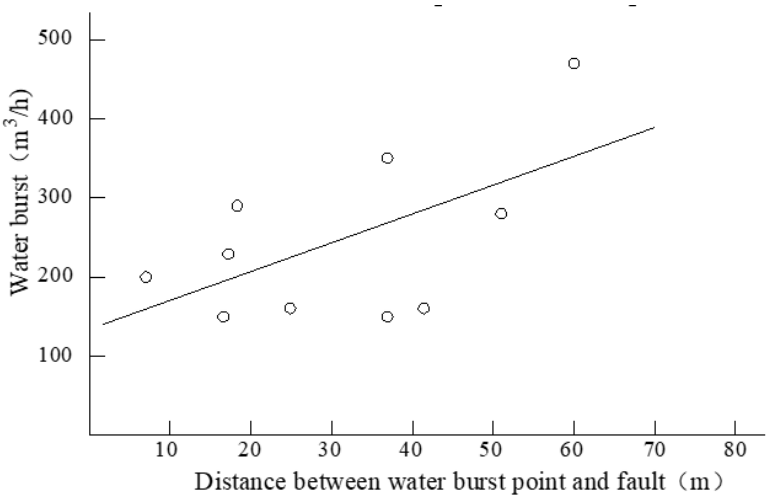

Figure 8. Relationship between water burst volume and the distance from the water burst point to the fault.

 doi:10.20944/preprints202506.0461.v1

q=3.8207X+128.39 (R^2=0.3742) (2)

Where q is the water burst, m^3/h; X is the distance from the water burst point to the fault, m.

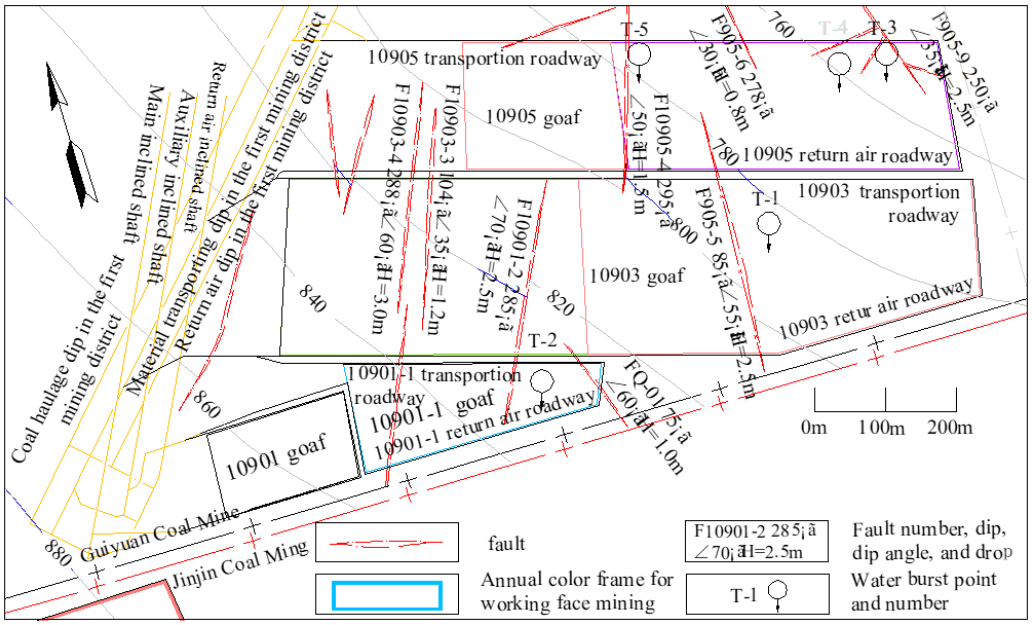

Figure 9. Planar relationship diagram between several water burst points and faults in the Guiyuan Coal Mine.

4. Study on the Water-Rich Characteristics of Changxing Formation Limestone After Mining Damage

4.1. The Water-Rich Characteristics of the Limestone in Its Original State

A total of 268 boreholes have been drilled in the limestone of Changxing Formation within the mining region. The maximum linear karst rate revealed by the boreholes was 0.8%. Locally developed karst caves are found in the limestone, with drilling revealing cave heights between 0.18 m and 8.74 m. Some caves are filled by yellow clay. Some boreholes penetrating this limestone leaked water, with a leakage rate of 17.5%. The depth of the leakage points is shallow at 367.4 m, and the lowest elevation is 922.16 m. The pumping test data from all coal mines in the mining region indicate that only one borehole (Linhua coal mine) in the Changxing Formation limestone has a specific capacity (q) of only 0.1418 L/m • s, the other boreholes range between 0.0000041 and 0.0127 L/m • s. The permeability coefficient K in the mining region was measured at 0.1079 m/d in only one borehole by the pumping test, and all others range between 0.0000026 and 0.004 m/d. Therefore, the Changxing Formation limestone is overall a weak water-abundance (permeable) aquifer [38,39], with poor connectivity of dissolution gaps and weak water conductivity. Karst has developed in the area of structural development, with good water abundance, and there may be a large amount of water inflow during production. The water inflow of initial mining face in various coal mine is relatively small, generally less than 30 m^3/h, which verifies the weakly water-rich characteristics of the Changxing Formation limestone. According to the data from the transient electromagnetic method of the roof implemented in the mining face of various coal mines in the mining region, in the absence of mining in the adjacent mining face of the upper section, indicating the limestone's general lack of water-bearing capacity. The lower sections of the 20915 and 20917 working faces of the Linhua coal mine have been fully mined out, and there is no goaf in the upper section. The transient electromagnetic method was used in the mine to detect the abnormal water-rich area on the roof of the two layers in the working face, and no significant water-rich anomalies was found in the Changxing Formation limestone. Afterward, 42 boreholes for exploration and drainage of the Changxing Formation limestone were drilled in the mine, but no water emerged from the exploration and drainage boreholes.

 doi:10.20944/preprints202506.0461.v1

On the basis of a comprehensive analysis, the Changxing Formation limestone is generally an aquifer with weak water yield potential under its original occurrence conditions, with poor connectivity of dissolution gaps and weak permeability. Karst is present at the location of structural development, with good water abundance, and water burst may have occurred during mining. The outcrops of Changxing Formation limestone are widely distributed across the mining region, making them susceptible to atmospheric precipitation recharge.

4.2. Water-Rich Characteristics of Changxing Formation Limestone After Mining Damage

After more than 20 years of continuous mining operation in some coal mines within the mining region, the recovery of the coal bed 9 near the shallow outcrop have been completed, and in some coal mines, the 4# or 5# coal bed have already been mined. A large goaf area has formed around the shallow coal bed outcrop in the mining region. The extensive mining-induced damage has resulted in a large-scale surface fracture zones. Some mines and the exposed Changxing Formation contain fractures with widths ranging from 0 to 2.3 m and extension lengths ranging from a few meters to more than 100 m. During the exploration of various coal mines in the mining region, the maximum width of the fissures in the Changxing Formation limestone exposed by drilling was 3 cm, and the maximum height of the karst cave reached 8.74 m. Mining-induced damage has further led to the development of internal fractures in the Changxing Formation limestone that connect the original dissolution fissures, karst caves, and fractures in the Changxing Formation limestone [1,4,6], thus forming a very large effective water storage space (Figure 10). With the massive infiltration of atmospheric precipitation, the Changxing Formation limestone on the goaf roof strata, under conditions of water storage, has gradually become the direct or indirect water-filling source for the stope across the mining area, and This damaged aquifer now serves as the direct water source for burstes during coal bed mining. The Changxing Formation limestone under shallow conditions serves as both a water storage space for infiltrated atmospheric precipitation and a supply channel to supply the stope below its elevation for atmospheric precipitation. During the period of water burst in the working face, the phenomena is typically accompanied by periodic roof weighting and exhibits a progressive evolution from dripping water to steady seepage and eventually water burst. Moreover, after the working faces are mined through the water burst points, the water inflow in the goaf gradually decreases and stabilizes. Water burst may occur again in the next working face or in special sections of this working face.

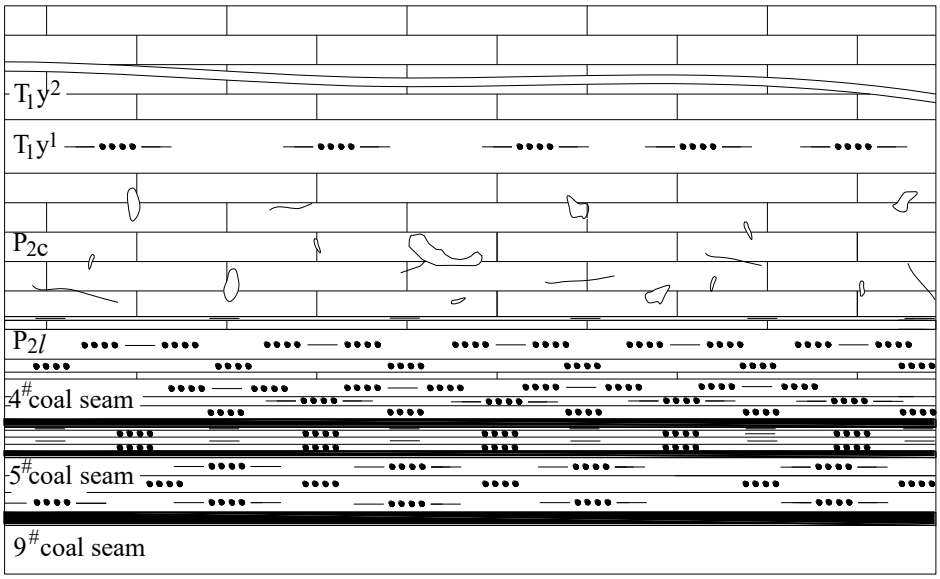

(**a**)

 doi:10.20944/preprints202506.0461.v1

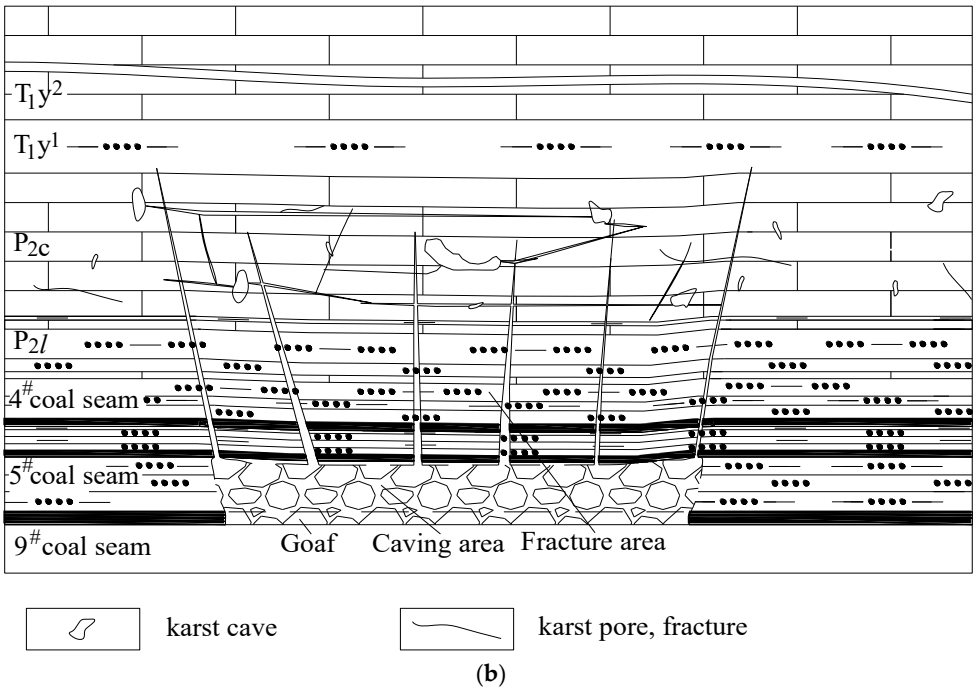

Figure 10. Status of the connection between dissolution fissures and karst caves before and after mining in the working face. **(a).** Status of the connection between dissolution fissures and karst caves before mining in the working face. **(b).** Status of the connection between dissolution fissures and karst caves after mining in the working face.

To investigate the characteristics of the water-rich changes in the limestone of Changxing Formation in the affected area after the coal bed mining, in Tenglong Coal Mine, Guiyuan Coal Mine, Linhua Coal Mine, and Anshenglongfeng Coal Mine, underground transient electromagnetic exploration work was carried out after the development of the lower section or adjacent working faces. These surveys aimed to explore the abnormal water-rich areas of the roof limestone of the working face. Among the areas, the abnormal water-rich area of the Changxing Formation limestone in the 2098 (east) mining face of the Linhua Coal Mine is particularly obvious. The 2098 mining face (east) is located on the east wing of the second mining district, with the upper section of the 2096 mining face (west), the 2094 working face, and the lower section of the 20910 working face already fully mined. This working face has a strike length of 482 m, the inclined length (width) is 150 m, and the coal bed thickness is 0.7–3.3 m. After the formation of the working face, transient electromagnetic detection was promptly carried out in the return airway, roadway, and cutting eye. Transient electromagnetic detection of the working face revealed the presence of four water-rich anomaly zones on the roof, i.e., YC1, YC2, YC3, and YC3 (Figure 11), all of which developed in the Changxing Formation aquifer, the spatial development characteristics of each water-rich anomaly area are shown in Table 5. The water-rich anomalous Zone 1 and water-rich anomalous Zone 2 are caused by the mining impacts of the 20910 and 2098 working faces. Zone 3 of the water-rich anomaly may be caused by the accumulation of water in karst caves developed in the Changxing Formation limestone. For example, in the Anshenglongfeng Coal Mine, the bottom gas drainage roadways of the 1903 and 1905 working faces were used as the drilling site (Figure 12), and four sets of seven drainage boreholes into the limestone aquifer of the Changxing Formation in the top plate of the 1903 goaf were drilled. The seven boreholes that exposed the Changxing Formation limestone all revealed the development of mining-induced fractures in the limestone. The longest and smallest fractures exposed by the boreholes ranged from 0.2 m to 1.0 m, respectively, and the typical range of fractures were between 0.2 and 0.5 m. The boreholes that revealed the limestone of the Changxing Formation all encountered water inflow, with a maximum water output reaching 50 m^3/h. The geological, hydrogeological, and transient electromagnetic data measured underground indicate that after mining damage, the Changxing

 doi:10.20944/preprints202506.0461.v1

Formation limestone has developed fractures within the rock mass, and the fractures are connected to the dissolution fissures and karst caves in the original rock. The limestone of Changxing Formation has formed a water storage space. Consequently, the limestone has become a supply source for mine water burst.

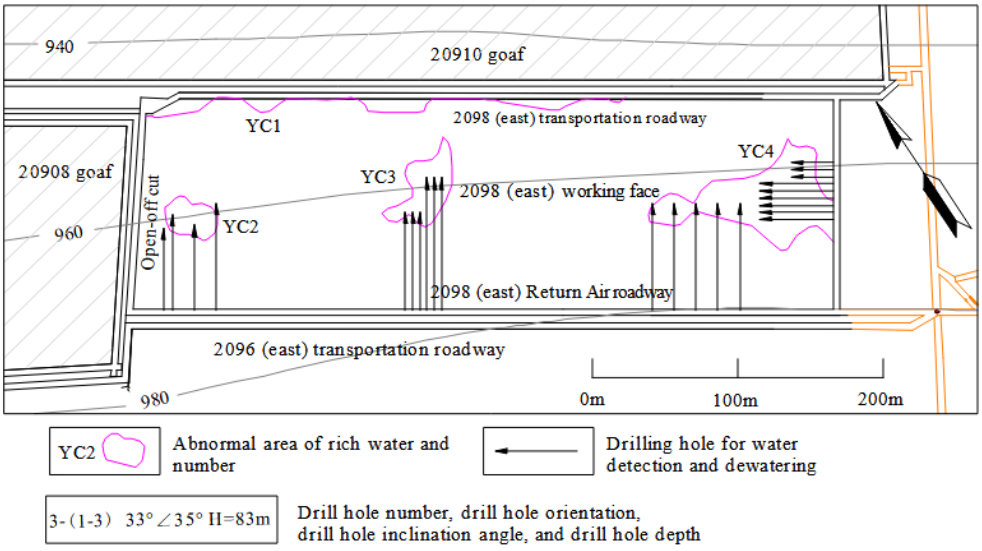

(a)

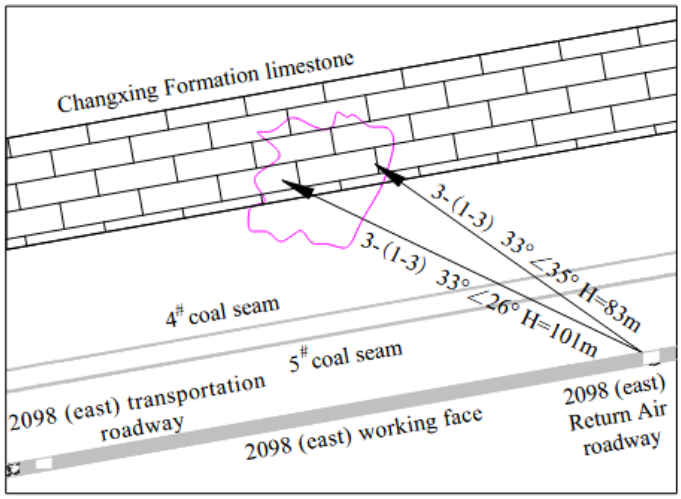

(b)

Figure 11. Sectional view of the anomalous water-rich area and YC3 water exploration borehole in the 2098 (east) working face. **(a).** Plan view of the water-rich anomaly zone and drainage borehole layout in the 2098 (East) working face. **(b).** Sectional view of exploration boreholes for water in the anomalous YC3 water-rich area of the 2098 (east) working face.

Table 5. Development characteristics of water rich anomaly areas.

Number of water rich anomaly Zone	Length（m）	Width（m）	Height（m）	Height of development within the Changxing Formation limestone (m)
1	326.3	13.1	37.8	32.6
2	36.1	31.5	38.5	22.3
3	63.9	48.0	34.4	20.2
4	131.7	79.3	21.6	18.5

 doi:10.20944/preprints202506.0461.v1

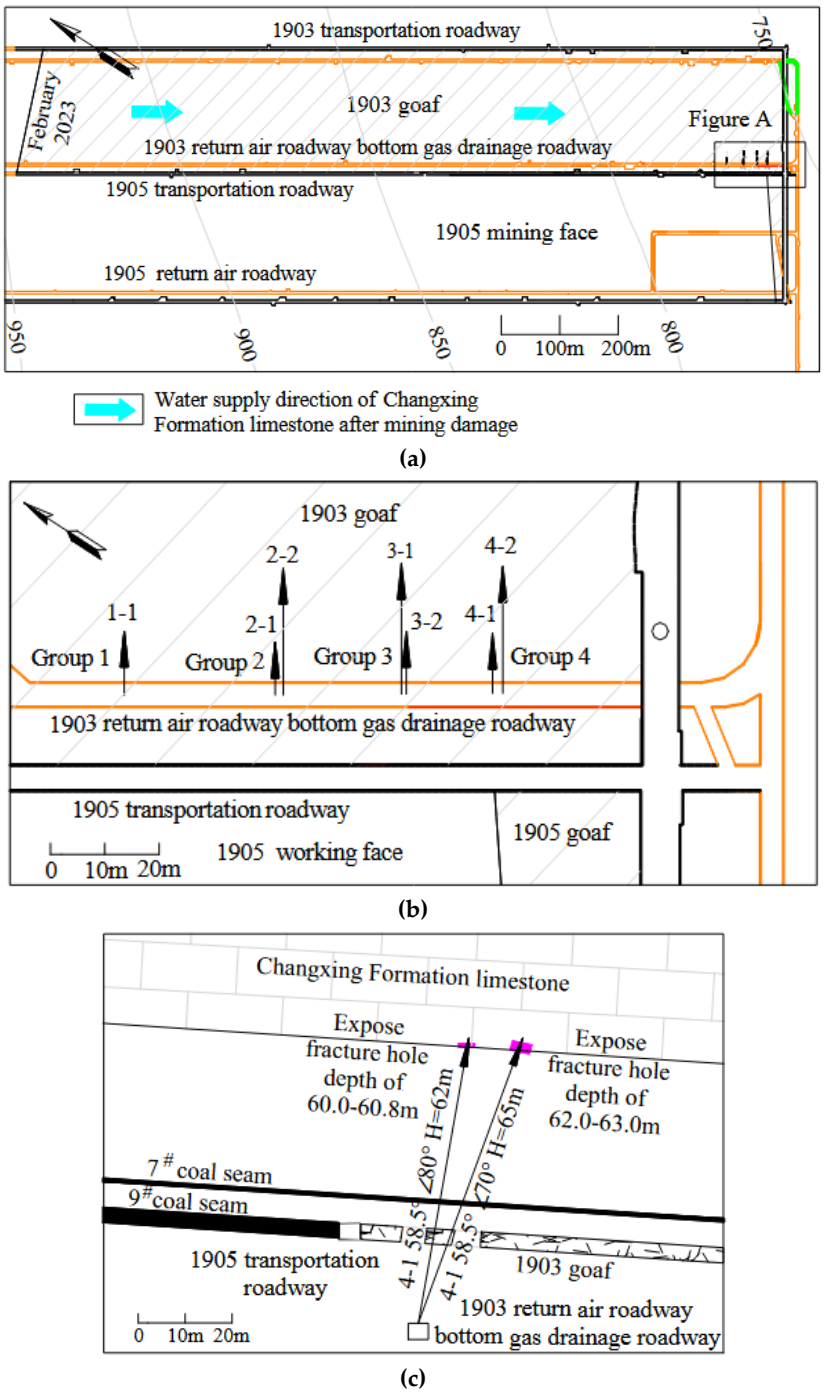

Figure 12. Diagram showing the drilling for detecting fractures in the Changxing Formation limestone after destruction by mining. **(a).** Planed layout of drill holes for the detection of fractures in the Changxing Formation limestone after destruction by mining. **(b).** Planned layout of boreholes for detecting fractures in the Changxing Formation limestone after destruction by mining (enlarged view of Figure A). **(c).** Section showing the fourth group of detection boreholes.

4.3. Variation Characteristics of Specific Yield After Mining Damage

The specific yield refers to the ratio of the volume of water released from an aquifer under the action of gravity to the volume of the medium. It is the ratio of the amount of water that is freely drained from a saturated aquifer per unit area under the action of gravity to the volume of the aquifer. It is an indicator for evaluating the performance of the water supply of aquifers [40–43]. If all the voids in the rock are filled with water, the water content is equal to the void content. However, in reality, owing to poor connectivity between the voids, a closed void that cannot accommodate water is formed, or there are bubbles in the void after filling, so the water content is usually less than the

 doi:10.20944/preprints202506.0461.v1

void content. The specific yield u is the ratio of the volume Vn of rock voids, and can accommodate water to the volume (V) of the rock, expressed as: u=Vn/V, which is expressed in percentages or decimals. In the process of mine production, the ratio of the static storage released by the aquifer to the volume of the aquifer, i.e., u=Qs/V, can be used to calculate the specific yield of the aquifer.

The voids in the Changxing Formation limestone after mining damage are composed of original dissolution fissures, karst caves, fractures, and newly formed mining-induced fractures. The first three are connected by fractures caused by mining damage, forming an effective water-bearing space for the Changxing Formation limestone to recharge the mine with water and establishing supply channels for shallow water sources. During the process of supplying the mining area with water from the Changxing Formation limestone aquifer, the initial water inflow originates from static storage and dynamic recharge, whereas the later inflow into the mining area is from dynamic water. The ratio of the static storage water released in the aquifer to the total volume of the limestone of the Changxing Formation forms the water yield of the Changxing Formation limestone. To more accurately predict the possible water burst volume and intensity of the next section of the working face, complete water burst data were collected from three pairs of mine working faces from the Anshenglongfeng Coal Mine, the Guiyuan Coal Mine, and the Lindonglongfeng Coal Mine, and the specific yields were calculated.

The 1903 working face is the first mining panel in Anshenglongfeng Coal Mine, and the adjacent 1905 working face is the second mining face of this coal mine. The water burst source of the 1905 working face was caused by the limestone water of the Changxing Formation in the roof of the goaf after the mining damage of the 1903 working face. Therefore, utilizing both the water burst volume of the 1905 working face and the volume of the limestone caused by mining damage on the goaf roof of 1903 working face, the specific yield of the mining-induced limestone aquifer of the Changxing Formation can be used to calculate. This result enables to evaluate the water-rich characteristics of the Changxing Formation limestone, and provide technical data for predicting water inflow in future working faces. Based on water burst volume and Changxing Formation limestone volume parameters (Table 6) from three pairs of working faces in different coal mines , the process of calculating the specific yield is as follows:

Table 6. Statistics of water burst and the volume fraction of the Changxing Formation limestone.

Mine	No. of the water burst working face	Water burst inflow (static replenishment quantity Qs) (m^3)	Supply goaf area (m^2)	Thickness of Changxing Formation limestone (m)	Changxing Formation limestone volume V (m^3)	Water burst time of the working face (year, month, day)	Latest production stoppage time of the goaf (year, month)
Ansheng longfeng Coal Mine	1095	101337	271290	38.37	10588444	2023.4.12	2023.2
Guiyuan Coal Mine	10901-1	76000	10630885	44.11	10635885	2019.2.25	2018.8
Lindonglong feng Coal Mine	5914	43260	195521	40.00	7820840	2020.3.24	2018.5

$$Q = Qs + Qd \quad (3)$$

$$Qs = Q - Qd \quad (4)$$

Thus:

$$u = \frac{Qs}{V} \quad (5)$$

 doi:10.20944/preprints202506.0461.v1

Where Q is the total water inflow at the water burst point, m^3; Qs is the static storage capacity of the aquifer, m^3; Qd is the dynamic recharge of the aquifer, m^3; u is the specific yield; and V is the volume of aquifer, m^3.

According to the data in Table 6, the specific yield of the Changxing Formation limestone in the goaf of the panel 1903 in Anshenglongfeng Coal Mine is 0.957%, that of the Changxing Formation limestone in the recharge area of the panel 10901-1 in Guiyuan Coal Mine is 0.715%, and that of the Changxing Formation limestone in the recharge area of the panel 5914 in Lindonglongfeng Coal Mine is 0.553%.

According to the analysis of data, it reveals the shorter the interval T (time unit：month, abbreviated as: M) between the water burst time and the end time of the mining face, the greater the specific yield, and vice versa (Figure 13). The magnitude of the specific yield is significantly related to the interval between the water burst time and the end time of the mining face corresponding to the overlying Changxing Formation limestone, and the two are exponentially correlated. The regression equation is as follows:

$u=1.0513d^{-0.2189}$ ($R^2=0.9293$) (6)

The correlation coefficient R is 0.964, indicating a high degree of correlation between the two parameters.

The water burst date at the panel 1095 in Anshenglongfeng Coal Mine is only 2 months after the end date of mining at the panel 1093. The specific yield of the Changxing Formation limestone is the highest, at 0.957%. The water burst date of the panel 5914 and the end date of the mining of the panel 5917 in Lindonglongfeng coal mine differ by 21 months. The specific yield of the Changxing Formation limestone is the lowest, at 0.553%. The water burst date of the panel 10901-1 in the Guiyuan Coal Mine differs from the completion date of the backfilling in the supply area by 4 months, then the specific yield of the Changxing Formation limestone is 0.715%, which is between the two mentioned above. These findings indicate that the Changxing Formation limestone has a natural tendency to close its fractures over time after destruction by mining. In addition, the sedimentation and filling of loess particles and other debris in the water source have reduced its effective water storage space. An increase in sedimentary particles not only causes poor water flow in the supply channel but also gradually decreases the water inflow in the goaf [4]. In addition, the loess particles that are deposited and filled in the cracks during this process are also the root cause of the collapse of loess slurries in some coal mines during the early stage of water burst [10].

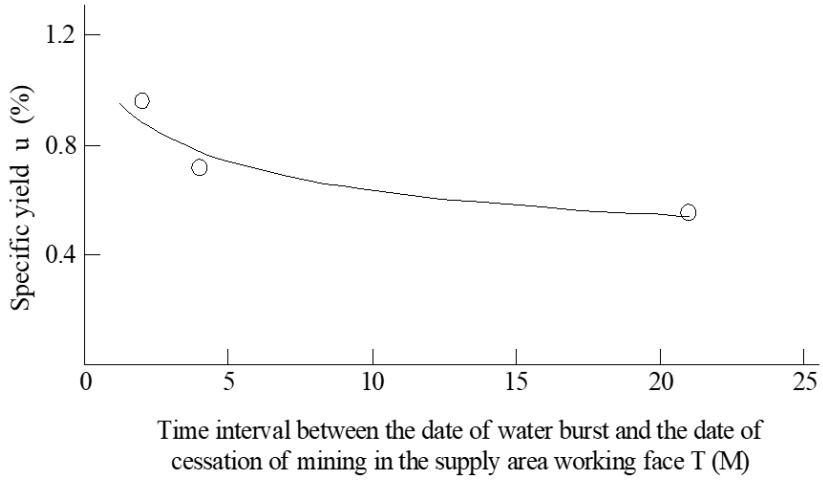

Figure 13. Curve related to the specific yield: the time interval between the date of water burst and the date of cessation of mining at the working face in the supply area.

5. Application of the Research Results

5.1. Design Optimization of the Working Face

 doi:10.20944/preprints202506.0461.v1

After the extraction of the uper section working face of the coal bed 9, the mining damage fractures and the primary dissolution fissures, karst caves, and fractures in the overlying Changxing Formation limestone strata in the goaf roof jointly formed a large effective water storage space. During the mining of the next section working face, when the water-conducting channel connect with the Changxing Formation limestone aquifer, water burst can occur in the working face. Before the water burst from the Changxing Formation limestone caused by mining damage, all coal mines in the Xinhua mining region adopted a downward arrangement of working faces. So that, the underground water stored in the Changxing Formation limestone caused by shallow working face damage could smoothly recharge the the roof Changxing Formation limestone in the lower section, leading to water burst in the next section of the mining face. After the completion of mining in the 2094, 2096, and 2098 working faces of Linhua Coal Mine, roof water burst occurred successively in the lower sections of the 20910 and 20912 working faces during the mining period. Afterwards, the mine changed the design of the working face by gradually adjusted the mining sequence, and transite from the downward mining face to the upward mining face, avoiding the phenomenon of water burst from the working face.For example, the upper limit working face 2096 (East) mined In 2023 after the completion of mining in the lower section of working faces 20910, 20912, 20914, etc., and no water burst occurred during the mining period of this working face.

5.2. Enhancement of the Disaster Resistance Capability of the Drainage System

Before the water burst occurred in the working face of each coal mine in the mining region, due to the normal water inflow of the working face being below 30m³/h, the drainage capacity of the drainage pump and drainage pipeline equipped normally in the working face was around 50m³/h. After the water burst, the transportation roadway of the working face was often flooded by the water inflow, causing the production of the working face to stop for a while. When designing the working face in the next section, each mine estimated the water inflow and water burst of the new mining face based on the water burst volume of the working face. Before water inrush occurred, the water inflow at working faces typically ranged between 20-30 m³/h. After water inrush incidents, the maximum water burst volume at working faces reached 80-800 m³/h. Therefore, based on the maximum burst volume, some mines predicted the water burst volume for the upcoming mining face by applying the upper stage mined area and specific yield, and combined with the hydrogeological analogy method. Accordingly, drainage equipment was installed to handle the predicted maximum burst volume. After the upgrade of the drainage system, each mining face in the mining area is generally equipped with 2-4 drainage pumps with drainage capacities from 130–520 m³/h. Drainage pipelines are generally installed with 2–3 pipes, with a single drainage pipeline diameter ranging from 150 to 200 mm. Four IS-125-100-250A single-stage centrifugal pumps with a rated flow rate of 187 m³/h are installed in the outer section of the roadway of the 5914 working face in the Lindonglongfeng Coal Mine. Four drainage pipes are installed in the roadway, including 2 pipes with a diameter of 200 mm and 2 pipes with a diameter of 150 mm. The total drainage capacity of the working face exceeds 700 m³/h, ensuring safe mining of the working faces. In the mine, the main drainage pump and drainage pipeline of the central water pump room were also renovated. After the renovation, two MD280-43 × 3 water pumps and two MD360-60 × 3 water pumps were installed in the central water pump room, and two DN350 mm main drainage pipelines were installed, greatly improving the disaster resistance of the mine.

5.3. Geophysical Exploration and Drilling Measures

In order to eplore the water-rich characteristics of the Changxing Formation limestone and predict roof water hazards in advance, in each coal mine carried out roof transient electromagnetic exploration and necessary exploration work were strictly carried out before excavation and mining in accordance with regulations. Through geophysical exploration, abnormal water-rich areas on roofs can be identified, and then drilling verification can be conducted. The drilling for verification must be designed according to the geophysical results, and the final depth of the drilling must exceed the

 doi:10.20944/preprints202506.0461.v1

abnormal area of the geophysical exploration of the Changxing Formation limestone. If water comes out of the boreholes in the geophysical anomaly area, it is necessary to increase the number of boreholes to dewater the aquifer and simultaneously expand the coverage of the drainage boreholes to ensure that the water in the Changxing Formation limestone is drained as cleanly as possible to avoid water burst during the coal mining and affect the normal production of the mine. For the dynamic recharge water in the drillhole, flexible hoses is used to divert water to a temporary water sump for centralized drainage. Drilling verification is carried out at the drillhole site, with dynamic supply water recharge in the working face, further draining the static storage of water in the Changxing Formation limestone. During the excavation of the working face roadway, at least one exploratory water borehole terminated within the limestone layer of the Changxing Formation. If water inflow is obversed in the boreholes, the additional boreholes should be increased, and transient electromagnetic detection should be carried out again. The integration of geophysical exploration and drilling measures has basically ensured the safe mining of mining faces, as demonstrated by the 2098 working face in Linhua Coal Mine mentioned above.

6. Conclusion

(1) The material simulation test and ground measurement data have verified that the water conducting fracture zone developed into the Changxing Formation limestone, leading to the failure of the Changxing Formation limestone. The height of the water conducting fracture zone in this karst mining area is not less than 25.78 times the mining height, significantly exceeding the empirical formula's calculated range of 13.0-15.8 times..

(2) After the mining damage of the Changxing Formation limestone, the mining damage fractures connected its primary dissolution fissures and karst caves, causing it to transform from a weakly water rich (permeable) aquifer to a water rich (permeable) aquifer and a water burst source of stope.

(3) The specific yield of Changxing Formation limestone after mining damage decreases with the increase of water burst time and the interval between the stoppage of mining in the supply area. The regression equation is $u=1.0513d^{-0.2189}$, a high degree of correlation between these variables.

(4) This finds provides theoretical basis and practical experience for water hazard prevention and control in mining areas (wells) under similar hydrogeological conditions.

Author Contributions: Conceptualization,Guosheng Xu; methodology, Xianzhi Shi and Ziwei Qian; validation, Guosheng Xu and Xianzhi Shi; investigation, Guosheng Xu and Xianzhi Shi; resources, Guosheng Xu; data curation, Ziwei Qian and Xianzhi Shi; writing-original draft preparation, Xianzhi Shi, Weiqiang Zhang; Paper revision and polishing, Guosheng Xu, Xianzhi Shi, Weiqiang Zhang; supervision, Xianzhi Shi; project administration, Guosheng Xu; funding acquisition, Guosheng Xu. Each author has read and approved the final version of the manuscript for publication.

Funding: This study was jointly funded by the innovation team of universities in Guizhou Province for mine water disaster prevention and control in the southwest karst area. (Guizhou Education Department [2023] 092), and Guizhou Provincial Basic Research Program (Natural Science) MS [2025] (No. 241).

Data Availability Statement: Data supporting the results of this study can be requested from the corresponding author when needed. All co authors declare that the content presented in this study is an original research achievement and has not been published in any journal, nor has it been submitted in whole or in part to any other journal for review.

Acknowledgments: All those acknowledged have agreed.

Conflflicts of Interest: The authors have no conflicts of interest to disclose.

 doi:10.20944/preprints202506.0461.v1

References

1. Li Bo, Wu Huang, Wu Qiang, et al. Prediction technology of mine water inflow based on entropy weight method and multiple nonlinear regression theory and its application. Geomech. Geophys. Geo-energ. Geo-resour. 2024,10(127), 1-13. https://doi.org/10.1007/s40948-024-00842-1.
2. Wang Haijun. Prediction of water inflow in Huoshaopu Coal Mine in Panxian basin, Guizhou Province. China Coal Geology. 2019, 31(7), 44-51.
3. Suo Jie, Qin Qirong, Wang Wenqiang, et al. Disastrous mechanism of water burst by karst roof channel in rocky desertification mining area in southwest China. Geofluids. 2022, 1-9. https://doi.org/10.1155/2022/7332182.
4. Shi Xianzhi, Zhang Weiqiang. Characteristics of an underground stope channel supplied by atmospheric precipitation and its water disaster prevention in the karst mining areas of Guizhou. Scientifc Reports. 2023, 13, 15892. https://doi.org/10.1038/s41598-023-43209-4.
5. Gong Xiaoyu, Li Bo, Yang Yu, et al. Construction and application of optimized model for mine water inflow prediction based on neural network and ARIMA model. Scientific Reports. 2025, 15, 2009. https://doi.org/10.1038/s41598-025-85477-2.
6. Li Zhenhua, Li Songtao, Du Feng, et al. Research on the development law of karst caves on water conducting fractures under the influence of mining in southwest karst mining areas. Coal Science and Technology. 2023, 51(7), 106-117.
7. Wang Yuliang, Kong Dezhong, Wu Guiyi, et al. Failure mechanism and movement characteristics of overlying strata in longwall mining face with thick aquifer. Rock Mechanics and Rock Engineering. 2024, 57, 6787-6809. doi: 10.1007/s00603-024-03929-z.
8. Xianzhi Shi, Guosheng Xu, and Shuyun Zhu. Water-filling characteristics and water source of weakly rich aater and weakly conducting water aquifers in the Changxing Formation after mining damages. Applied Sciences. 2024, 14(10), 4018. ttps://doi.org/10.3390/app14104018.
9. Jin Mingfang, Yao Xiaoshuai1, Zhang Wanpeng, et al. Technical study on formation mechanism and comprehensive prevention and control of separated layer water in Changxing Formation of Qianbei Coal Field [J]. Coal Technology. 2023, 42(12), 128-132.
10. Zheng Gang. Analysis of the formation mechanism of water and gangue collapse accidents in Tenglong Coal Mine, Guizhou Province. China Coal Geology. 2024, 36 (03), 43-46+5.
11. Jin Xu, Lulin Zheng, Hong Lan. et al. Research on an identification model for mine water inrush sources based on the HBA-CatBoost algorithm. Scientifc Reports. 2024, 14, 23508 . https://doi.org/10.1038/s41598-024-74417-1.
12. Shuyuan Xu, Yongbo Zhang, Hong Shi, et al. Physical simulation of strata failure and its impact on overlying unconsolidated aquifer at various mining depths. Water. 2018, 10(5), 650. https://doi.org/10.3390/w10050650.
13. Lele Xiao, Li Fan, Niu Chao, et al. Evaluation of water inrush hazard in coal seam roof Based on the AHP-CRITIC composite weighted method. Energies. 2023, 16(1), 114. https://doi.org/10.3390/en16010114.
14. Shun Liang, Xuepeng Zhang, Fahong Ke, et al. Evolution of Overlying Strata Bed Separation and Water Inrush Hazard Assessment in Fully Mechanized Longwall Top-Coal Caving of an Ultra-Thick Coal Seam. Water. 2025, (17)6: 850. https://doi.org/10.3390/w17060850.
15. Jin Dewu，Li Chaofeng，Liu Yingfeng，et al. Characteristics of roof water hazard of coal seam in Huanglong Coalfield and key technologies for prevention and control. Coal Geology & Exploration. 2023, 51(1), 205-213. doi: 10.12363/issn.1001-1986.22.10.0754.
16. Shi Xianzhi, Zhu Shuyun, Zhang Weiqiang. Study on the mechanisms and prevention of water inrush events in a deeply buried high-pressure coal seam-a case study of the Chensilou Coal Mine in China. Arab J Geosci. 2019, 12, 614. https://doi.org/10.1007/s12517-019-4824-z.
17. Wu Yanjun. Key technology for double-layer hole treatment of water inrush disasters in high pressure aquifers. Coal Engineering. 2024, 56 (08), 86-92.
18. Yue Li, Yunpeng Zhang, Yajie Ma, et al. Risk analysis of coal seam floor water inrush based on GIS and combined weight TOPSIS method. All Earth. 2024, 36(1), 2410108. https://doi.org/10.1080/27669645.2024.2410108.

 doi:10.20944/preprints202506.0461.v1

19. Zhang Weijun. Analysis of water drilling technology for exploring top plate sandstone in the 1013 working face of Yushuquan Coal Mine. Shandong Industrial Technology. 2015, 21, 41-41 .
20. Jinjun Li, Zhihao He, Chunde Piao, et al. Research on subsidence prediction method of water-conducting fracture zone of overlying strata in coal mine based on grey theory model . Water. 2023, 15(23), 4177. https://doi.org/10.3390/w15234177.
21. Jiabo Xu, Daming Yang, Zhenquan Zhang,et al. Study on fracture evolution and water-conducting fracture zone height beneath the sandstone fissure confined aquifer. Sustainability. 2024, 16, 6006. https://doi.org/10.3390/su16146006.
22. Lulin Zheng, Xiaokun Wang, Hong Lan, et al. Study of the development patterns of water-conducting fracture zones under karst aquifers and the mechanism of water inrush. Scientifc Reports, 2024, 14, 20790. https://doi.org/10.1038/s41598-024-71853-x.
23. Li Bo, Wei Tao, Liu Zijie. Construction of evaluation index system for water abundance of karst aquifers and risk assessment of water inrush on coal seam roof in Southwest China. Journal of China Coal Society. 2022, 47(S1), 152-159.
24. State Administration of Work Safety, National Coal Mine Safety Supervision Bureau, National Energy Administration, et al. Regulations for the setting of coal pillars and coal mining in buildings, water bodies, railways, and main mines(Coal Industry Press, 2017).
25. Mark Alexander Van Dyke, Peter Zhang, Heather Dougherty, et al. Identifying Longwall-Induced Fracture Zone Height Through Core Drilling. Mining, Metallurgy & Exploration. 2022, (39), 1345-1355. https://doi.org/10.1007/s42461-022-00622-z.
26. Li Yachao Research on the law of water inrush disasters caused by water conducting faults during deep buried tunnel excavation. Henan University of Technology, Jiaozuo, 2023.
27. Mu Wenping, Wu Xiong, Deng Ruochen, et al. Mechanism of Water Inrush Through Fault Zones Using a Coupled Fluid–solid Numerical Model: A Case Study in the Beiyangzhuang Coal Mine, Northern China. Mine Water Environ. 2020, (39), 380–396. https://doi.org/10.1007/s10230-020-00689-4.
28. Zhong Zuliang, Shen Zhuo, Qiao Hongyan, et al. Study on Mechanism of Water and Mud Inrush in Deep-Buried Large-Section Tunnel Crossing Water-Rich Fault Fracture Zone. Rock Mech Rock Eng. 2025, (58), 1147–1164. https://doi.org/10.1007/s00603-024-04176-y.
29. Guangli Zhu, Shuli Wang, Wenquan Zhang, et al. Research on the mechanism and evolution Law of delayed water inrush caused by fault activation with mining. Water. 2023, 15(24), 4209. https://doi.org/10.3390/w15244209.
30. Shao Jianli, Zhang Qi, Zhang Wenquan. Evolution of mining-induced water inrush disaster from a hidden fault in coal seam floor based on a coupled stress–seepage–damage model. Geomech. Geophys. Geo-energ. Geo-resour. 2024, 10 (78), 1-21. https://doi.org/10.1007/s40948-024-00790-w.
31. Sun Wenbin, ZHang Jiyang, Wang Xiao, et al. Staged sensing method of fault sudden water based on gray correlation analysis. China Safety Science Journal. 2024, 34(7), 63-70.
32. Hongjin Sun, Rui Pan, Junwei Li. Research on the mechanism of fault activation and water inrush across variable coal pillar widths. Dvances in Civil Engineering. 2024, 8557425. https://doi.org/10.1155/2024/8557425.
33. Long Tang, Shihao Tu, Hongsheng Tu, et al. Interaction law between mining stress and fault activation and the effect of fault dip angle in longwall working face. Scientific Reports. 2024, 14, 25654. https://doi.org/10.1038/s41598-024-75878-0.
34. Zhou Lu, Liu Enlightenment, Jiang Zihao, et al. Analysis of surrounding rock damage and fault activation characteristics in coal seam mining [J]. Modern Mining. 2019, 35 (06), 140-142.
35. Rentao Gou, Chengyu Jiang, Yong Liu, et al. Study on fractal characteristics of evolution of mining-induced fissures in karst landform. Energies. 2022, 15(15), 5372. https://doi.org/10.3390/en15155372.
36. Tianwei Lan, Yonghao Liu, Yongnian Yuan. et al. Determination of mine fault activation degree and the division of tectonic stress hazard zones. Scientifc Reports. 2024, 14, 12419. https://doi.org/10.1038/s41598-024-63352-w.

 doi:10.20944/preprints202506.0461.v1

37. Yanpeng He, Qingxiang Huang, Li Ma. Study on the mechanism and control of strong ground pressure in the mining of shallow buried close-distance coal seam passing through the loess hilly region. Geomech. Geophys. Geo-energ. Geo-resour. 2025, 11-14. https://doi.org/10.1007/s40948-024-00929-9.
38. Qingping Lu, Cuiwei Zhao, Huiyu Huang. Comparative study on the temporal and spatial evolution of the ecosystem service value of different karst landform types: A case study in Guizhou Province, China. Applied Sciences. 2022, 12(24), 12801. https://doi.org/10.3390/app122412801.
39. National Coal Mine Safety Supervision Bureau. Detailed Rules for Water Prevention and Control in Coal Mines (Coal Industry Press, 2018).
40. J.M. Vouillamoz, F.M.A. Lawson, N. Yalo, et al. The use of magnetic resonance sounding for quantifying specific yield and transmissivity in hard rock aquifers: The example of Benin. Journal of Applied Geophysics. 2014, 107, 16-24. https://doi.org/10.1016/j.jappgeo.2014.05.012.
41. Xu Liang, Zhenghui Xie, Maoyi Huang. A new parameterization for surface and groundwater interactions and its impact on water budgets with the variable infiltration capacity (VIC) land surface model. Journal of Geophysical Research. 2003, 108(D16), 8613. doi:10.1029/2002JD003090, D16.
42. Meizhao Lv, Zhongfeng Xu, Zongliang Yang. A comprehensive review of specific yield in land surface and groundwater studies. Journal of Advances in Modeling Earth Systems. 2021, 13, e2020MS002270. https://doi.org/10.1029/2020MS002270.
43. Ndifreke I. Udosen, Nyakno J. George. Evaluation of specific retention, specific yield, and storage-dependent drainability efficiency in a coastal milieu via geo-electrical technology. Water Practice & Technology. 2024, 19(9), 3654. DOI: 10.2166/wpt.2024.208.